PROCEEDINGS OF ISAP '92, SAPPORO, JAPAN

ASYMPTOTIC ANALYSIS OF HIGH-FREQUENCY PROPAGATION IN A TROPOSPHERIC SURFACE DUCT

Yasuhiko Sakaguchi and Toyohiko Ishihara Department of Electrical Engineering, National Defense Academy, Hashirimizu, Yokosuka, 239, Japan

1.INTRODUCTION

High-frequency propagation beyond the limit of direct visibility is of special interest for practice and theory[1],[2]. The troposphere, which provides a channel for electromagnetic waves, can generally be described by a modified refractive index that varies vertically as well as laterally. Because the problem scale is large at high-frequency and for long propagation distances, direct numerical modeling is either inefficient or not feasible. Therefore, effective algorithm must be developed.

Analytical modeling of high-frequency propagation in elevated or surface ducts by normal trapped and leaky modes is inconvenient because of the large number of modes that may be required[3]. Moreover, synthesis with normal modes, does not directly model the physics of the propagation process in those domains where that process is essentially ray-like.

It appears that geometrical ray fields with caustic correction, when required, furnish an efficient model away from the strong trapping regime near the lower boundary, with a few trapped modes included in the boundary layer near the bottom. We have shown previously that the hybrid ray-mode representation is numerically accurate when source and observation points are located in the boundary layer of a bilinear modified refractive index height profile[4],[5].

However, the ray fields fail in the transition region surrounding the critical trajectory that grazes the duct boundary beyond which leakage occurs. The approach to grazing and the ray splitting beyond have been accounted for uniformly by a group of trapped and leaky modes whose local plane wave congruences are closely aligned with the grazing trajectory. Thus, by incorporating this mode group self-consistently into the previous format, we have derived the new hybrid ray-mode representation that can accommodate sources and observation points located arbitrarily inside the duct or on the duct[4],[5].

In the present study, the method of geometrical optics for the fields in a surface duct is extended to account for the fields above the surface duct and in the refraction shadow of geometrical rays[6]. Included are ray-optical, trapped and leaky modes, and diffracted rays, and various combinations of these. Numerical comparisons reveal the validity and utility of the various alternative field representations.

2. FORMULATION AND ASYMPTOTIC REPRESENTATIONS

We limit our discussion to high-frequency propagation in and above a bilinear tropospheric duct excited by a vertical electric dipole located in the duct. The earth's surface is described by a surface impedance Zs [1]. It is convenient to utilize a cylindrical coordinate system to describe a tropospheric wave propagation excited by the vertical source over a curved earth. The curvature of the earth is taken into account by modifying the index of refraction of the atmosphere. The modified index of refraction is given by m(z)=n(z)+z/a, where n(z) is the index of refraction at the height z and a is the radius of the earth. The modified refractive index M(z) is defined as $M(z)=(m(z)-1)\times 10^6$.

A bilinear modified refractive index (M(z)) profile, which has the duct

boundary at the height zi and various ray trajectories radiated from the source Q are shown in Fig.1(a) and Fig.1(b), re- Z_i spectively. The grazing ray which becomes horizontal at the duct boundary or at the height of minimum refractive index may be refracted downward and upward directions. A refraction shadow is formed by the grazing ray and the caustics of trapped rays. Rays without the reflection at the duct boundary can not reach the observation points in the refraction shadow. When the vertical electric dipole is located at Q(r',z') in the cylindrical (r,ϕ,z) coordinate system, the magnetic and electric fields are specified in that system by the components H_{ϕ} and E_{r} , E_{z} , re-

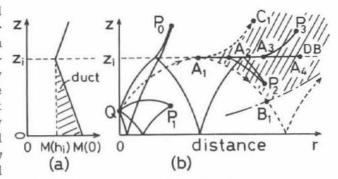


Fig. 1 Physical configurations.

(a) Bilinear modified refractive index profile and (b) the trajectories of trapped ray, reflected ray, transimitted ray, and diffracted ray. Also shown are the grazing ray(--->), a refraction shadow(shaded region), the caustic(---), and the duct boundary located at the height z=zi.

DB:duct boundary.

spectively(Fig.1). All field components can be derived from the z-component of Hertz vector or the relevant dipole source Green's function G(r,r'), which satisfies the inhomogeneous wave equation: $(\nabla^2 + k_0^2 m^2(z))G(r,r') = -\delta(r-r')$, with the radiation condition and the impedance boundary condition[1],[4]. Here k_0 is the wavenumber in free space.

In the previous paper, we derived the normal mode expansion, the ray expansion, and the hybrid ray-mode expansion from the integral representation of the Green's function[4],[5]. However, the asymptotic formulas developed so far are restricted to the fields in a geometrically illuminated region in the surface duct. Here, we will obtain the asymptotic formulas of the fields above the surface duct and in the refraction shadow.

2.1 Geometrical ray representation

Various rays arriving at the observation point P_0-P_2 in Fig.1(b) may be constructed directly from the conventional eikonal and transport equations [7]. Each ray that emerges from the source Q(0,z') at the angle θ_0 measured from the positive z-axis may be given in the following form.

$$G \sim \frac{e \, x \, p \, [\, i \, \phi_{QP}]}{4 \pi \sqrt{r}} \left\{ \frac{\alpha^{\, 2}}{m^{\, 2} \, (z \,) - \alpha^{\, 2}} \right\}^{1/4} \left\{ \frac{\Delta \, \rho}{\Delta \, \theta_{\, 0}} \right\}^{-1/2} \\ \times \left\{ \begin{array}{c} \left(\Gamma_{\, o} \right)^{\, N} \left(\Gamma_{\, i} \right)^{\, L} & \text{(ray reflected at the duct boundary)} & \text{(la)} \\ \left(\Gamma_{\, o} \right)^{\, N} \cdot \left\{ e \, x \, p \, (-i \, \pi \, / 2) \right\}^{\, L} & \text{(trapped ray)} & \text{(lb)} \\ \left(\Gamma_{\, o} \right)^{\, N} \left(\Gamma_{\, i} \right)^{\, L - 1} T_{\, i} & \text{(transmitted ray)} & \text{(lc)} \end{array} \right.$$

Where a=m(z')sin θ_0 . Δr is the distance in r-direction from the observation point P(r,z), located on the axial ray, to the paraxial ray leaving the source at the angle $\theta_0 + \Delta \theta_0$. Φ_{QP} is the phase change along the trajectory. $[\Gamma_0,N]$ and $[\Gamma_i,L]$ denote [reflection coefficient, number of reflection] at the earth's surface and the duct boundary, respectively. T_i is the transmission coefficient at the duct boundary.

2.2 Diffracted ray representation

For a particular value of θ_0 , the ray grazes the duct boundary. One may imagine that the grazing ray QA_I (see Fig.1) splits at the point A_I into the

rays A_1B_1 , A_1C_1 and $A_1A_2A_3A_4$, continuing along the duct boundary and giving rise to a continuous set of diffraction rays A_2P_2 , A_3P_3 , and so on. For example, the diffracted ray $QA_1A_2P_2$ may be given in the following form.

$$G \sim \frac{e \times p[i |\phi_{QA_1} + k(z_i)d + \phi_{A_2P_2}]}{4\pi\sqrt{r} \{m^2(z') - m^2(z_i)\}^{1/4} \{m^2(z) - m^2(z_i)\}^{1/4}} \sum_{m} D_m^2 e^{-\alpha_m d}$$
(2)

Where Φ_{QA_1} and $\Phi_{A_2P_2}$ are the phase changes over the portions QA_1 and A_2P_2 , $k(z_i$) is the wavenumber at the height z_i , d is the horizontal distance between A_1 and A_2 . D_m and α_m are the diffraction coefficient and the attenuation coefficient of the m-th mode for the bilinear refractive index profile. These coefficients are determined from the normal mode expansion obtained from the integral representation of the Green's function[4],[5] . By expanding normal mode solution asymptotically with respect to $k(z_i)$ as $k(z_i) \to \infty$ and comparing the result with geometrical optics, one may determine D_m and α_m .

3.NUMERICAL RESULTS

We implement numerical calculations of the fields by using the asymptotic representations derived in Section 2. Their utility is assessed by numerical comparisons with the exact reference solutions. Reference solutions for the various examples considered below have been generated from the normal mode expansion retaining 107 modes[5]. The duct parameters and operating frequency are(cf.Fig.1): duct height $z_1=200m$, M(0)=65.7m, $M(z_1)=31.4m$, dM(z)/dz=157m/km for $z>z_1$, surface impedance $Z_s=0$, and f(frequency)=9GHz.

When the sources are placed away from the boundary layer, the fields in an illuminated region may be approximated by geometrical optics. We have shown in Fig.2 that the result calculated from the ray representation (Fig.2(a)) agrees pretty well with the reference solution (Fig.2(b)). However, the mode series reference solution becomes successively more slowly convergent as the observation point moves to the upper direction. The discrepancy between two results near the height 250 m is due to the truncation of the modes series.

Fig.3 shows the field magnitude versus height. The field magnitudes in Fig.3(a) in the refraction shadow(RS) are evaluated from the combination of the diffracted ray in Eq.(2) and the reflected ray in Eq.(1a). While the fields in the boundary layer(BL) near the bottom and in the illuminated region above BL are calculated from the hybrid ray-mode representation[4]

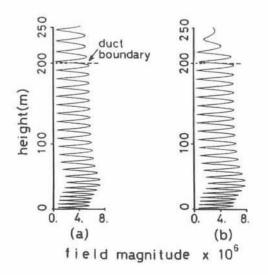


Fig. 2 Field magnitude versus height at the horizontal range 30km, with the source located 40m above the earth's surface. Observer passes through the observation points Po and P, in Fig. 1(b). Fig. 2(a) is obtained from the ray representation in Eq. (1). Two trapped rays (the direct ray (N=0, L=1) and the ray once reflected at the earth's surface(N=1, L=1)) and transmitted rays (N=0, L=1) and (N=1, L=1) are used in and above the surface duct, respectively.

Fig. 2(b):reference solution.

and from the ray representation (two trapped rays), respectively. Fig.4 shows the field magnitude versus horizontal range. In Fig.4(a), the ray representation is applied in the illuminated region and the combination of diffracted rays and reflected rays is applied in the refraction shadow(RS). The asymptotic results in Fig.3(a) and Fig.4(a) agree well with the reference solutions in Fig.3(b) and Fig.4(b), respectively.

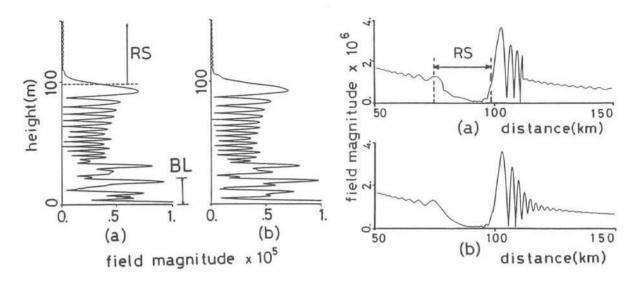


Fig. 3 Field magnitude distribution curves along the vertical observation line located at the horizontal range 95 km. The observation point P₂ in Fig. 1(b) is located on this line. Source height: Z'=0(m). (a) Asymptotic representation and (b) reference solution.

Fig. 4 Field magnitude distribution curves along the horizontal observation line located at the height 110m. The observation point P_x in Fig. 1(b) is located on this line. Source height: Z'=0(m). (a) Asymptotic representation and (b) reference solution.

4.CONCLUSION

We have studied an asymptotic approach to representing high-frequency propagation in and above a bilinear tropospheric duct excited by a vertical electric dipole. Numerical comparisons with the reference solution calculated from the normal mode expansion have confirmed the accuracy and utility of the new asymptotic formulations involving geometrical rays, diffracted rays, and various combinations of these.

REFERENCES

[1]J.R.Wait, Electromagnetic Waves in Stratified Media, New York, Pergamon, 1962, pp.107-137, 341-363.

[2]H.V.Hitney, R.A.Pappert and C.P.Hattan, Radio Sci., vol.13,no.4,pp.669-675, 1978.

[3]R.H.Ott, Radio Sci., vol.16, no.6, pp.1149-1154, 1981

[4]T.Ishihara and L.B.Felsen, IEEE Trans. Antennas and Propagat., vol.39, no.6, pp.780-788, 1991.

[5]T.Ishihara and L.B.Felsen, IEEE Trans. Antennas and Propagat., vol.39, no.6, pp.789-797, 1991.

[6]B.D.Seckler and J.B.Keller, The Journal of the Acoust. Soc. of America, vol.31, no.2, pp.192-205, 1959.

[7]L.B.Felsen and N.Marcuvitz, Radiation and Scattering of Waves, New Jersey, Prentice-Hall, 1973, Chaps.2,3 and 5.